

University of Arkansas, Fayetteville

ScholarWorks@UARK

Microelectronics-Photonics Faculty
Publications and Presentations

Microelectronics-Photonics

6-8-2021

Understanding Diffusion and Electrochemical Reduction of Li⁺ Ions in Liquid Lithium Metal Batteries

Witness Martin

University of Arkansas, Fayetteville

Yang Tian

University of Arkansas, Fayetteville

Jie Xiao

University of Arkansas, Fayetteville, jjexiao@uark.edu

Follow this and additional works at: <https://scholarworks.uark.edu/micropub>



Part of the [Electromagnetics and Photonics Commons](#)

Citation

Martin, W., Tian, Y., & Xiao, J. (2021). Understanding Diffusion and Electrochemical Reduction of Li⁺ Ions in Liquid Lithium Metal Batteries. *Journal of the Electrochemical Society*, 168 (6), 060513. <https://doi.org/10.1149/1945-7111/ac0647>

This Article is brought to you for free and open access by the Microelectronics-Photonics at ScholarWorks@UARK. It has been accepted for inclusion in Microelectronics-Photonics Faculty Publications and Presentations by an authorized administrator of ScholarWorks@UARK. For more information, please contact scholar@uark.edu, uarepos@uark.edu.

OPEN ACCESS

Understanding Diffusion and Electrochemical Reduction of Li^+ Ions in Liquid Lithium Metal Batteries

To cite this article: Witness Martin *et al* 2021 *J. Electrochem. Soc.* **168** 060513

View the [article online](#) for updates and enhancements.

You may also like

- [Nanoscale reorganizations of histone-like nucleoid structuring proteins in *Escherichia coli* are caused by silver nanoparticles](#)
Mead Alqahtany, Prabhat Khadka, Isabelle Niyonshuti *et al.*
- [Energy efficient graphite–polyurethane electrically conductive coatings for thermally actuated smart materials](#)
A Bhattacharyya, E Dervishi, B Berry *et al.*
- [Alternative stable states and hydrological regime shifts in a large intermittent river](#)
Sam Zipper, Ilinca Popescu, Kyle Compare *et al.*

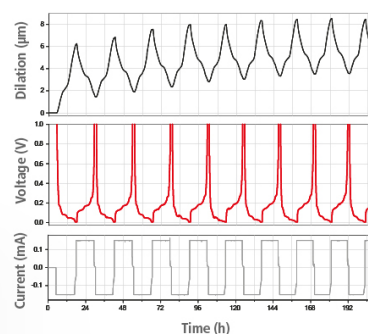
Watch Your Electrodes Breathe!

Measure the Electrode Expansion in the Nanometer Range with the ECD-4-nano.

- ✓ Battery Test Cell for Dilatometric Analysis (Expansion of Electrodes)
- ✓ Capacitive Displacement Sensor (Range 250 μm , Resolution ≤ 5 nm)
- ✓ Detect Thickness Changes of the Individual Half Cell or the Full Cell
- ✓ Additional Gas Pressure (0 to 3 bar) and Temperature Sensor (-20 to 80° C)



EL-CELL[®]
electrochemical test equipment



See Sample Test Results:



Scan me!

Download the Data Sheet (PDF):



Scan me!

Or contact us directly:

+49 40 79012-734

sales@el-cell.com

www.el-cell.com



Understanding Diffusion and Electrochemical Reduction of Li⁺ Ions in Liquid Lithium Metal Batteries

Witness Martin,^{1,=} Yang Tian,^{1,=} and Jie Xiao^{2,3,*,#,z} 

¹Microelectronics-Photonics Program, Graduate School and International Education, University of Arkansas, Fayetteville Arkansas 72701, United States of America

²Chemistry and Biochemistry Department, University of Arkansas, Fayetteville, Arkansas 72701, United States of America

³Pacific Northwest National Laboratory, Richland Washington 99354, United States of America

Lithium metal has drawn significant interest as an anode material for next generation lithium (Li) batteries. However, due to its propensity to form dendrites in commonly used electrolytes during repeated cycling, it has not yet been commercialized in secondary batteries. The formation of a Li protrusion is determined by the relative speed of Li⁺ ions being reduced and how fast they can be replenished in the vicinity of electrode. However, it is very difficult to quantify such kinetic parameters of Li⁺ ion in different electrolytes, not mentioning the identification of the desired electrolyte recipe to mitigate Li dendrite formation. Herein, we use microelectrodes to study the growth mechanism of electroplated Li by measuring the Li⁺ diffusion coefficient (D_{Li}) and exchange current density (i_0) in different electrolytes. The different Li morphologies formed on microelectrodes are well correlated to their diffusion rate and electrochemical reduction speed on the electrode, providing a fast electrochemical tool to screen compatible electrolytes for Li metal batteries.

© 2021 The Author(s). Published on behalf of The Electrochemical Society by IOP Publishing Limited. This is an open access article distributed under the terms of the Creative Commons Attribution 4.0 License (CC BY, <http://creativecommons.org/licenses/by/4.0/>), which permits unrestricted reuse of the work in any medium, provided the original work is properly cited. [DOI: 10.1149/1945-7111/ac0647]



Manuscript submitted January 26, 2021; revised manuscript received April 12, 2021. Published June 8, 2021. *This was paper 477 presented at the Dallas, Texas, Meeting of the Society, May 26–May 30, 2019.*

Supplementary material for this article is available [online](#)

Rechargeable lithium metal batteries are considered as one of the most promising next-generation battery technologies because of the low density (0.534 g cm⁻³) and high gravimetric capacity (3680 mAh g⁻¹) of lithium metal.^{1–3} However, lithium is reactive in almost all liquid electrolytes, producing a passivation layer known as the solid electrolyte interface (SEI) which covers the surface of the Li metal electrode.⁴ In addition, similar with all electroplated metals, Li prefers to form dendritic microstructures in the liquid cell due to the presence of convection.⁵ In some instances, the dendritic Li may grow strong enough to penetrate through the separator membrane and cause an internal short-circuit which could potentially lead to additional performance drawbacks and serious safety hazards. Li protrusions have increased surface area compared to the Li foil, which accommodate more side reactions on these newly exposed surfaces, generating more SEI at the expense of the electrolyte. The presence of SEI layers interferes with the homogeneous distribution of the electrical field on the Li metal anode which further induces uneven growth of Li during the plating process. Additionally, the SEI layer partially breaks down when Li is stripped and new SEI forms during the Li deposition process.⁶ The continuous accumulation of SEI results in the constant consumption of electrolyte and produces “dead” Li deposits when some Li particles are coated by thick SEI layers and become disconnected from the Li anode.⁷ These fundamental issues are just some of the many challenges that still impede the large-scale deployment of rechargeable lithium metal batteries.

To overcome the barriers of using the lithium metal anode, the intrinsic reasons that stimulate the uneven growth of the Li metal anode need to be considered. Even without the SEI layer, the electrochemical deposition of other metals such as Ag, Cu or Zn, which is intrinsically related to the mass transport of metal ion species in the electrolyte is rarely smooth⁸ in the absence of brighteners or levelers. In the electrolyte solution, the diffusion rate of Li⁺ ions arriving at the anode surface from the bulk electrolyte (similar to the electroplating process) plays a key role in the formation of Li dendrites.⁹

The fast transport of the plating ions (Li⁺) arriving at the slowly (low current density) plated electrode (Li) leads to the formation of a smooth and shiny metal layer during electroplating, while the slow transport of the plating Li ions arriving at the rapidly plated electrode (high current density) leads to the formation of fibrous Li dendrites. This explains why the opportunity of forming dendritic Li is largely increased at high current densities because Li⁺ ions are being reduced to Li much faster. If Li⁺ cannot be replenished timely, a high concentration gradient will form and induce the growth of Li towards the bulk electrolyte. The use of highly concentrated electrolytes increases the abundance of Li ions at the electrode vicinity and thus reduces the Li⁺ concentration gradient in the same electrolyte solution with regular 1–1.2 M molarity and helps to smoothen out the Li dendrites,^{5,10,11} assuming the same current density is utilized for the electrochemical reaction. Both cation transport in the liquid electrolyte and the reaction rate of the electrochemical reactions need to be considered in understanding Li dendrite growth.

In this work, we integrate different electrochemical measurement approaches to quantify the kinetic properties of Li⁺ ion diffusion and reaction in various electrolytes in an attempt to develop an electrochemical tool to rapidly screen through a variety of electrolyte recipes. A microelectrode is used in the electrochemical measurements with the explicit purpose to exclude the interference from convection and for fast signal response which provides new insights in understanding and comparing various electrolytes.

Experimental

Nickel (Ni) microwire with a purity of 99.98%, a diameter of 125 μm, and coated with 5 μm of Polyimide (PI) were purchased from GoodFellow and used as is. These are herein referred to as the Ni microelectrode. The copper (Cu) microelectrodes were made in-lab using uncoated 25 μm Cu microwire with a purity of 99.95% also sourced from Goodfellow. The design process of the Cu microelectrode is shown in Fig. S1 (available online at stacks.iop.org/JES/168/060513/mmedia) in the supplemental section. Lithium perchlorate (LiClO₄), lithium hexafluorophosphate (LiPF₆), lithium bis(fluorosulfonyl)imide (LiFSI) and lithium bis(trifluoromethanesulfonyl)imide (LiTFSI) salts, as well as ethylene carbonate (EC), dimethyl carbonate (DMC), propylene carbonate (PC), fluoroethylene carbonate (FEC), Triethyl phosphate (TEP), and bis(2,2,2-trifluoroethyl) ether (BTFE)

⁼These authors contributed equally to this work.

*Electrochemical Society Fellow.

^zE-mail: jjexiao@uark.edu

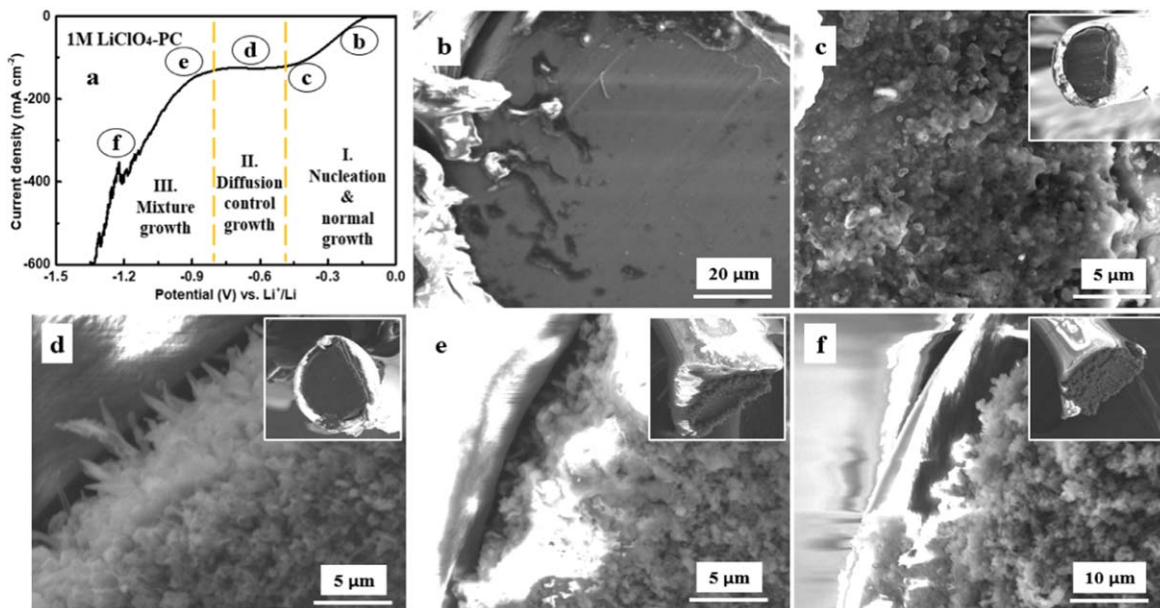


Figure 1. (a) LSV curve obtained by a 125 μm microelectrode. (b)–(f) SEM images of lithium-ion deposition at different potential on a 125 μm microelectrode in 1 M $\text{LiClO}_4\text{-PC}$, potential step from 1 V to -1.5 V vs Li^+/Li at 23 $^\circ\text{C}$ and a scan rate of 130 mV s^{-1} .

solvents were purchased from BASF corporation and used as received. Electrolytes were prepared by mixing each salt with either EC-DMC (v/v, 1:1) or PC or TEP-BTFE (v/v, 1:1). For the preparation of electrolytes with additives, FEC (5% vol.) was added to the EC-DMC or PC as an additive solvent. Electrolytes were prepared in an inert Ar gas environment inside a glovebox.

Two different electrochemical cell setups that allowed for the control of the distance between the working electrode and the counter electrode were used. The design of these electrochemical cells is shown in the supplemental information (Fig. S2). Electrochemical measurements were performed using an electrochemical station manufactured by CH Instruments, Inc. (Model: CHI 660e). Using this instrument, the following test profiles were created and utilized: Linear Sweep Voltammetry (LSV) between 1 V and -1.5 V vs Li^+/Li at a scan rate of 130 mV s^{-1} ; Cyclic Voltammetry (CV) from 1 V to -0.4 V vs Li^+/Li , at a scan rate of 100 mV s^{-1} ; Chronoamperometry (CA) was performed at -0.015 V vs Li^+/Li . The surface morphology of the working electrodes was observed by scanning electron microscopy (SEM).

Results and Discussion

Ni and Cu microelectrodes (see experimental part for more details) have been used to determine kinetic parameters such as the exchange current density (i_0) and the diffusion coefficient (D_{Li}) of Li^+ in different electrolyte systems. The former reflects how fast Li/Li^+ redox reacts, while the latter provides information of the diffusion rate of Li^+ ions in different electrolytes and therefore how fast to replenish the plated Li^+ ions near the electrode.

Diffusion of Li^+ in bulk electrolytes.—The Ni microelectrode has been used to quantify the kinetic parameters of Li deposition. By limiting the deposition surface area to the micro scale, the effects of convection in the electrolyte, usually observed in macroelectrodes (coin and pouch cells), is negated.^{12,13} Due to its size, the diffusion controlled process can be induced in the local vicinity of the microelectrode's deposition surface even at time lengths shorter than Sand's Time.¹⁴ This fast signal response makes it ideal for testing the kinetic behavior of the electrolyte.

Linear sweep voltammetry was applied on the Ni microelectrode in a 1 M $\text{LiClO}_4\text{-PC}$, at a scan rate of 130 mV s^{-1} between 1 V and -1.5 V, as shown in Fig. 1a. The morphologies of deposited lithium

on the microelectrode tip at different potentials are displayed in Figs. 1b–1f. Looking at Fig. 1a, region I represents the onset of the nucleation and charge transfer stage. During this stage the current density increases with potential growth, and the morphology of the lithium metal is relatively smooth on the microelectrode (Fig. 1b) due to minimized interference from convection, exhibiting no sharp Li dendrite growth. The tail end of Region I (point c) is signified by a slow growth of the current density, indicating a reduction in the concentration of Li^+ ions at the microelectrode surface, i.e., concentration gradient is being strengthened in this region. At this point some protrusions begin to evolve (Fig. 1c). Once the potential reaches region II in Fig. 1a, the diffusion-controlled region, the concentration gradient of Li^+ across the diffusion region has risen considerably to a limit that the concentration of Li^+ ions reaches its minimum, therefore the current is determined by an equilibrium between the arrival of Li^+ and their reduction to Li at the microelectrode surface, explaining why the current density remains constant during this region. At this point Li dendrites are aggressively induced to form propagations towards the bulk electrolyte (Fig. 1d) where more Li^+ are available. The current density only remains constant for a while before it continues to increase again. This is due to the fact that Li metal, once deposited into sufficiently large format (Fig. 1e), can be considered as a new current collector on which Li metal can be continuously plated and establish new concentration gradients on those Li tips. Formation of SEI layers on the increasing Li surfaces also consumes electrons which count into the measured current. Deposited Li therefore exhibits a very porous structure extending towards different directions (Fig. 1f) after passing the diffusion-controlled region.

As similarly demonstrated by,¹⁵ D_{Li} , a measure of the ease of Li^+ diffusion through the electrolyte, was determined by applying the chronoamperometry (CA) technique using the Cu microelectrode. D_{Li} was then calculated using Eq. 1, where α represents the radius of the microelectrode tip, and S is the slope as shown in Fig. S3. For a detailed explanation on how this technique was applied, please refer to the supporting information.

$$D_{\text{Li}} = \frac{\pi \alpha^2}{16 S^2} \quad [1]$$

The same method was used to measure D_{Li} of Li^+ ions in different electrolytes which are listed in Fig. 2. The SEM images of Li

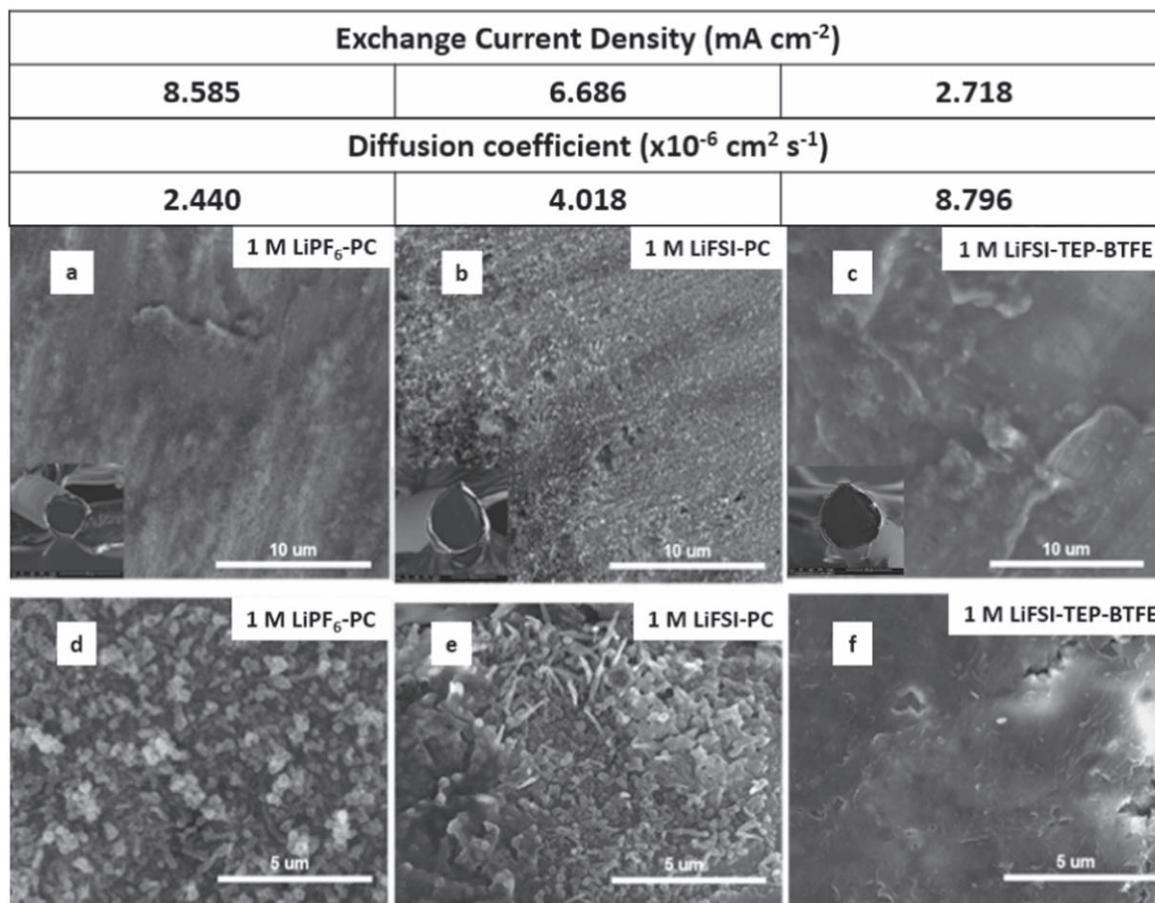


Figure 2. SEM images of lithium deposition on a microelectrode in (a) 1 M LiPF₆-PC, (b) 1 M LiFSI-PC, and (c) 1.2 M LiFSI-TEP-BTFE by LSV, potential step from 1 V to -0.4 V vs Li⁺/Li at 23 °C and a scan rate of 130 mV s⁻¹. (d)–(f) are respective amplified SEM images in the diffusion-controlled state.

deposits in Fig. 2 were selected from diffusion controlled regions during which Li dendrites are growing aggressively by using the same microelectrode measurement technique. The morphologies of the lithium deposits in Fig. 2 are closely related to the Li⁺ diffusion coefficient in the various electrolytes. For the purpose of ensuring that the measurements of D_{Li} were performed correctly, the measured diffusion coefficient of the 1 M LiClO₄-PC electrolyte was compared to values found in literature. There was strong agreement between the measured value of $2.049 \times 10^{-6} \text{ cm}^2 \text{ s}^{-1}$ and those found in multiple literature sources which ranged between $2.6\text{--}2.9 \times 10^{-6} \text{ cm}^2 \text{ s}^{-1}$.^{16–18} A similar phenomena has been discovered in other electrolytes as well. These results can be found in Fig. S5 in the supplement information. In general, a higher D_{Li} usually leads to a smoother deposition of Li on the electrode even during the diffusion controlled region because the fast diffusion of Li⁺ can adequately replenish the consumed Li⁺ at the electrode surface in a timely manner, thus smoothening the concentration gradient in the vicinity of the electrode. This phenomenon can be witnessed in Fig. 2. For the electrolyte in which D_{Li} is around $2 \times 10^{-6} \text{ cm}^2 \text{ s}^{-1}$ (Figs. 2a and 2d), the majority of plated Li forms a largely granular and unsmooth surface suggesting a quick depletion of Li⁺, and thus a strong concentration gradient established in the vicinity of the electrode surface. As D_{Li} increases to around $4 \times 10^{-6} \text{ cm}^2 \text{ s}^{-1}$ the morphology tends towards a less granular structure (Figs. 2b and 2e), suggesting a lower concentration gradient due to the faster arrival of Li⁺ at the electrode surface.

Keeping with the trend, the 1.2 M LiFSI-TEP-BTFE electrolyte (Figs. 2c and 2f), with the highest D_{Li} at $8.796 \times 10^{-6} \text{ cm}^2 \text{ s}^{-1}$ results in the smoothest deposition. The electrochemically plated Li in this system is very smooth even at the diffusion-controlled area where

concentration gradient is the strongest. The LSV curves of the electrolytes in Fig. 2 can be found in Fig. S6 in the supplemental information. Of the studied electrolytes, the 1 M LiClO₄-PC electrolyte system reached the diffusion-controlled at the lowest overpotential, and resulted in a highly dendritic morphology. This is consistent with the expected outcome that a low overpotential results in a lower nucleation density and limited deposition sites, leading to unsmooth growth.

Electrolyte viscosity also impacts D_{Li} . Table I compares the viscosity and D_{Li} of four electrolytes of similar concentration but different salts in a PC solvent, as well as single electrolyte comprised of PC and fluoroethylene carbonate (FEC) as a solvent additive. These exhibited a viscosity in the range of 2.6 to 3.22 mPa s. The lower viscosity resulted in a higher D_{Li} . The exception here however is the 1 M LiPF₆ + 5% FEC electrolyte. The addition of FEC led to an increase in D_{Li} despite a relatively higher viscosity. This can be attributed to FEC's effect on the solvation of Li⁺. This is consistent with work conducted by Ren et al.¹⁹ which shows that the use of an FEC additive leads to a smoother Li deposition. This confirms the indirect proportionality between D_{Li} and viscosity.

Plating rate of Li: exchange current densities of Li⁺/Li redox reactions.—Assuming the electroplating rate of Li occurs at a similar speed in all electrolytes, a higher D_{Li} is always favored by the electrolyte for plating smooth Li electrochemically. However, redox reaction rates between Li⁺ and Li also vary in different electrolytes because the derived SEI layers on Li surfaces affect the reaction rate across the interface. If Li⁺ is being reduced too quickly, a fast diffusion of Li⁺ may still not be able to “refill” the consumed Li⁺ near electrode surface leading to the evolution of strong

Table I. Tabulated diffusion coefficient, viscosity and exchange current density values of the various PC-based electrolytes.

Solvent	Lithium Salt	Diffusion Coefficient ($\times 10^{-6}$)	Viscosity (cP)	Exchange Current Density (mA cm^{-2})
PC	1 M LiFSI	4.018	2.62	6.686
	1 M LiTFSI	4.263	2.60	7.389
	1 M LiPF ₆	2.440	2.89	8.585
	1 M LiClO ₄	2.049	3.22	11.023
	1 M LiPF ₆ + 5% FEC	5.885	3.17	14.880

concentration gradients. Therefore, Tafel plot analysis (Fig. S4), was used to quantify the exchange current of Li⁺/Li redox in various electrolytes. The detailed measurement steps and calculations can be found in the supplementary information. Table I is a summary of the five PC-based electrolytes studied. A detailed summary of all examined electrolytes is available in Table SI in the supplementary information.

The exchange current density is the bi-directional (net-zero) current flow to maintain the equilibrium of both species during the reaction. It is a representation of the rates of oxidation and reduction between species at the equilibrium electrode. This was determined by applying cyclic voltammetry measurements using the Ni microelectrode. A higher exchange current density represents a faster reaction at the microelectrode surface meaning not much overpotential is needed to drive the electrochemical reaction to happen. A ranked comparison of all the electrolytes studied is listed in Table SI. For 1.2 M LiFSI-TEP/BTFE, the exchange current density (i_0) is lowest at 2.718 mA cm^{-2} , while D_{Li} is highest among all the electrolytes. The lower i_0 of Li⁺/Li redox in TEP/BTFE-based electrolyte needs a higher overpotential to drive the reaction, as reflected by Fig. S6d. A higher deposition overpotential is known to promote the nucleation rate of metals during electroplating²⁰ which will lead to less coarse surfaces of plated metals. Coupled with the relatively faster Li⁺ diffusion from the bulk TEP/BTFE electrolyte, the end result is the smooth deposition of Li on the microelectrode, consistent with the observations in Figs. 2c and 2f and previously reported results.^{3,21} By comparison, the measured i_0 was relatively similar across electrolytes of the same solvent of PC (Table I). This indicates that while the anion of the lithium salt has an effect on the rate of the reaction occurring at solvation boundary, its influence is not as significant as that of the solvent (Table SI). From this observed phenomenon it can be understood as that the inner Helmholtz layer on the electrode surface is still dominated by the polarized solvent molecules. Accordingly, the derived SEI layers which alter i_0 are determined more by the solvent.²² Only when the electrolyte concentration increases, do the anions start to participate more in the formation of SEI layers.^{23,24}

When designing an electrolyte to pair with Li metal, ideally an electrolyte with a high D_{Li} and a low i_0 should be sought because this ensures that there is always an adequate supply of Li⁺ at the electrode surface to prevent/suppress dendrite formation. However, in reality a very low i_0 will need high polarization to drive the plating process which will induce more electrolyte decomposition at low potentials. The presence of SEI did complicate the application of a single electrochemical tool. But a general rule of thumb is that, if the electrolyte does not generate highly resistant SEI layers covering the Li, a higher D_{Li} and a moderate i_0 is always beneficial.

Conclusions

The kinetic parameters, diffusion coefficient (D_{Li}) and exchange current density (i_0), of different electrolytes were measured using microelectrodes to understand the different morphologies of electroplated Li in these systems. The interlinked relationships between D_{Li} and i_0 are found to crucially dictate the relative speed of Li⁺ ions transport in electrolyte and how fast they are reduced to Li metal,

well explaining the observed Li morphologies. The microelectrode tools can be used as facile methods to fast-screen electrolytes for use in Li metal batteries and many other similar metal batteries, providing a fast screening approach for developing liquid electrolytes for future battery technologies.

Acknowledgments

The authors acknowledge the support from the National Science Foundation (NSF) under grant no. CBET-1748279. J.X. also acknowledges the support from Arkansas Research Alliance.

ORCID

Jie Xiao  <https://orcid.org/0000-0002-5520-5439>

References

- X.-B. Cheng, R. Zhang, C.-Z. Zhao, and Q. Zhang, "Toward safe lithium metal anode in rechargeable batteries: a review." *Chem. Rev.*, **117**, 10403 (2017).
- D. Lin, Y. Liu, and Y. Cui, "Reviving the lithium metal anode for high-energy batteries." *Nat. Nanotechnol.*, **12**, 194 (2017).
- S. Chen, J. Zheng, L. Yu, J. Xiao, J. Liu, and J. Zhang, "High-efficiency lithium metal batteries with fire-retardant electrolytes." *Joule*, **2**, 1548 (2018).
- Y. He, X. Ren, Y. Xu, M. H. Engelhard, X. Li, J. Xiao, J. Liu, J. Zhang, W. Xu, and C. Wang, "Origin of lithium whisker formation and growth under stress." *Nat. Nanotechnol.*, **14**, 1042 (2019).
- J. Xiao, "How lithium dendrites form in liquid batteries." *Science*, **366**, 426 (2019).
- C. Niu et al., "Self-smoothing anode for achieving high-energy lithium metal batteries under realistic conditions." *Nat. Nanotechnol.*, **14**, 594 (2019).
- B. Wu, S. Wang, J. Lochala, D. Desrochers, B. Liu, W. Zhang, J. Yang, and J. Xiao, "The role of the solid electrolyte interphase layer in preventing Li dendrite growth in solid-state batteries." *Energy Environ. Sci.*, **11**, 1803 (2018).
- Z. Ahmad and V. Viswanathan, "Stability of electrodeposition at solid-solid interfaces and implications for metal anodes." *Phys. Rev. Lett.*, **119**, 056003 (2017).
- M. S. Chandrasekar and M. Pushpavanam, "Pulse and pulse reverse plating—conceptual, advantages and applications." *Electrochim. Acta*, **53**, 3313 (2008).
- P. Bai, J. Li, F. R. Brushett, and M. Z. Bazant, "Transition of lithium growth mechanisms in liquid electrolytes." *Energy Environ. Sci.*, **9**, 3221 (2016).
- J. Qian, W. A. Henderson, W. Xu, P. Bhattacharya, M. Engelhard, O. Borodin, and J. Zhang, "High rate and stable cycling of lithium metal anode." *Nat. Commun.*, **6**, 6362 (2015).
- M. W. Verbrugge and B. J. Koch, "Microelectrode investigation of ultrahigh-rate lithium deposition and stripping." *J. Electroanal. Chem.*, **367**, 123 (1994).
- D. R. Baker and M. W. Verbrugge, "An analytic solution for the microdisk electrode and its use in the evaluation of charge-transfer rate constants." *J. Electrochem. Soc.*, **137**, 3836 (1990).
- H. J. S. Sand, "III. On the concentration at the electrodes in a solution, with special reference to the liberation of hydrogen by electrolysis of a mixture of copper sulphate and sulphuric acid." *Lond. Edinb. Dublin Philos. Mag. J. Sci.*, **1**, 45 (1901).
- G. Denuault, M. V. Mirkin, and A. J. Bard, "Direct determination of diffusion coefficients by chronoamperometry at microdisk electrodes." *J. Electroanal. Chem. Interfacial Electrochem.*, **308**, 27 (1991).
- K. Nishikawa, Y. Fukunaka, T. Sakka, Y. H. Ogata, and J. R. Selman, "Measurement of LiClO₄[sub 4] diffusion coefficient in propylene carbonate by moiré pattern." *J. Electrochem. Soc.*, **153**, A830 (2006).
- A. Ehrl, J. Landesfeind, W. A. Wall, and H. A. Gasteiger, "Determination of transport parameters in liquid binary lithium ion battery electrolytes." *J. Electrochem. Soc.*, **164**, A826 (2017).
- M. W. Verbrugge, B. J. Koch, and E. W. Schneider, "Mass transport in lithium-battery solvents." *J. Appl. Electrochem.*, **30**, 269 (2000).
- X. Ren, Y. Zhang, M. H. Engelhard, Q. Li, J.-G. Zhang, and W. Xu, "Guided lithium metal deposition and improved lithium coulombic efficiency through synergistic effects of LiAsF₆ and cyclic carbonate additives." *ACS Energy Lett.*, **3**, 14 (2018).

20. K. I. Popov, S. S. Djokic, and B. N. Grgur, *Fundamental Aspects of Electrometallurgy* (Springer, Boston, MA) 1st ed., 3, 29 (2002), (<http://site.ebrary.com/id/10053322>).
21. J. Xiao et al., "Understanding and applying coulombic efficiency in lithium metal batteries." *Nat. Energy*, **5**, 561-568 (2020).
22. K. Xu, "Nonaqueous liquid electrolytes for lithium-based rechargeable batteries." *Chem. Rev.*, **104**, 4303 (2004).
23. L. Suo, O. borodin, T. Gao, M. Olguin, J. Ho, X. Fan, C. Luo, C. Wang, and K. Xu, "'Water-in-salt' electrolyte enables high-voltage aqueous lithium-ion chemistries." *Science*, **350**, 938 (2015).
24. Y. Yamada, K. Furukawa, K. Sodeyama, K. Kikuchi, M. Yaegashi, Y. Tateyama, and A. Yamada, "Unusual stability of acetonitrile-based superconcentrated electrolytes for fast-charging lithium-ion batteries." *J. Am. Chem. Soc.*, **136**, 5039 (2014).